Magnetic Circular Dichroism Spectra of Divalent Lanthanide Ions in Calcium Fluoride

H. A. WEAKLIEM, C. H. ANDERSON, AND E. S. SABISKY

RCA Laboratories, Princeton, New Jersey 08540

(Received 19 June 1970)

The broad-band spectra of most of the divalent lanthanide ions in calcium fluoride were studied with circularly polarized light in magnetic fields at liquid-helium temperatures. Large field- and temperature-dependent anisotropies were found in the bands of ions having an odd number of electrons, all of whose states have Kramers degeneracy. A variety of effects are seen for ions having an even number of electrons, ranging from zero as in $CaF_2:Er^{2+}$ to the large, complex effects in $CaF_2:Dy^{2+}$. The magnetic linear dichroism (MLD) of both Dy^{2+} and Eu^{2+} were also measured. The magnetic circular dichroism (MCD) effects of the photochromic ions La^{2+}, Ce^{2+}, Gd^{2+}, and Tb^{2+} are similar to each other and are only briefly described. This study is primarily concerned with the nonphotochromic ions, whose spectra are due to transitions between the opposite-parity configurations $4f^n$ and $4f^{n-1}\,5d$. These ions all have the ground configuration $4f^n$. The magnetic dichroism effects are discussed in terms of the symmetry properties of the lanthanide ion. The large magneto-optic effects are the result of large spin-orbit coupling and predominantly totally symmetric vibronic coupling. Since the MCD and MLD effects are large throughout entire bands, they may be conveniently used in a variety of optical pumping experiments and may serve to detect changes in level populations.

I. INTRODUCTION

Crystals of CaF_2, SrF_2, and BaF_2 containing divalent lanthanide ions have been produced and studied in these laboratories during the past several years. The 2+ oxidation state is an uncommon one for most lanthanides, and for many of them it was first observed in these crystals.[1,2] There are strong absorption bands and the crystals are highly colored. Extensive studies on the absorption and emission spectra, electron paramagnetic resonance (EPR) spectra, and laser properties of these crystals have been done both here and in other laboratories.

We are primarily concerned with the intense, broad bands of the divalent lanthanides in CaF_2 in this paper, and with how they are affected by the application of a magnetic field. We have measured the magnetic circular dichroism (MCD) of most of the divalent lanthanides in CaF_2. The magnetic linear dichroism (MLD), also known as the Voigt effect, of $CaF_2:Eu^{2+}$ and $CaF_2:Dy^{2+}$ has also been measured and will be discussed. These studies have enabled us to confirm or deduce the ground- and excited-state configurations and to determine the symmetry species of some of the broad-band excited states. Most of the discussion is concerned with the general principles of how the various types of crystal impurity states contribute to the magneto-optical effects, and conversely how one may use the measured induced magnetic dichroism to deduce transition assignments.

The visible and ir $CaF_2:Ln^{2+}$ spectra contain intense, broad absorption bands as well as sharp absorption and emission lines. Most of the lines are a result of $4f\rightarrow 4f$ transitions between states of the $4f^n$ configuration. The bands are usually the result of parity-allowed (Laporte) electric dipole transitions between states of the $4f^n$ and $4f^{n-1}\,5d$ configurations which are separated by only a few thousand wave numbers. Crystals of CaF_2 containing either La, Ce, Gd, or Tb after reduction may exist in two or more metastable states and can be switched by light of different frequencies.[3] We shall only make passing reference to these photochromic crystals, and shall concentrate on those reduced crystals having a single stable spectrum.

Relatively little is known about the states of $4f^{n-1}\,5d$, particularly in the presence of crystal fields. In the stable nonphotochromic crystals, the divalent lanthanide occupies an alkaline-earth ion position in the crystal and therefore has cubic O_h symmetry.[4,5] In the $4f^{n-1}\,5d$ configuration, the $5d$ electron is split by an estimated several thousand wave numbers into the crystal-field e_g and t_{2g} components, e_g having the lower energy. Each of these crystal-field orbitals is coupled to the states of the well-shielded $4f^{n-1}$ core. The resulting states may be expected to be strongly coupled to vibrations through the large radial extension of the $5d$ electron. Since the states of $4f^n$ are well shielded, the electron-vibrational (vibronic) coupling is weak; therefore the equilibrium positions of the ions of the lattice may be quite different between the $4f^n$ and $4f^{n-1}\,5d$ configurations. Transitions between these configurations involve many phonon excitations in order to achieve the lattice readjustment and thus are broadened. That is to say, the spectral bands show large Frank-Condon shifts as a result of very different potential energy surfaces between electron configurations $4f^n$ and $4f^{n-1}\,5d$. The situation is in some ways analogous to that of the transition-metal ions in crystals, in which transitions between crystal-field configurations having different occupation numbers of e_g and t_{2g} orbitals are usually seen as broad bands.

Magneto-optical studies were undertaken in order to learn more about the electronic and vibronic coupling of the states of $4f^{n-1}\,5d$, and to investigate the use of magnetic-induced dichroism for optical pumping experiments.[6] An applied magnetic field may cause the crystal

eigenstates to split and interact and this, in general, causes a difference between the spectra for right and left circularly polarized light propagating in the field direction. The complementary Faraday effect—the rotation of the plane of polarization of light directed along the magnetic field—occurs because of the difference between the (real) refractive indices for right and left circularly polarized light.

The earliest Faraday rotation and MCD studies were done on systems having line spectra, including extensive work on trivalent rare-earth ions. Within the past few years the MCD and magnetic optical rotation (MOR) spectra of broad bands of transition-metal ions and color centers in alkali halides have been studied. The magneto-optical studies, with particular emphasis on inorganic systems, have been discussed and reviewed by Buckingham and Stephens.[7] There has been relatively little work done on the divalent lanthanides. The Faraday rotation and MCD of the 4011-Å line of $SrF_2:Eu^{2+}$ and of the 4130-Å line of $CaF_2:Eu^{2+}$ was measured and discussed by Shen.[8] The MLD of $CaF_2:Eu^{2+}$ has been reported[9] and there have been brief notes on the MOR and MCD of $CaF_2:Ho^{2+}$ [10,11] and the MOR of $CaF_2:Dy^{2+}$.[12] The MCD of several of the red lines of $CaF_2:Sm^{2+}$ have been analyzed by Margerie.[13] The MOR[8] of $CaF_2:Tm^{2+}$ has been measured and the MCD was discussed earlier by us.[6] Optical pumping experiments utilizing the MCD of $CaF_2:Tm^{2+}$ have also been described and this system has been operated as an optically pumped maser[14] by utilizing the MCD of one of the bands.

We shall present the MCD of the broad bands of most of the stable divalent lanthanides in CaF_2 as well as the MLD of $CaF_2:Eu^{2+}$ and $CaF_2:Dy^{2+}$. It is convenient to group the divalent lanthanides into three classes. First, there are the ions having odd-numbered f^n ground configurations. The magnetic dichroism has large anisotropies, and has strong temperature and field dependence. Second, there are the ions having even-numbered f^n ground configurations. The magnetic dichroism effects range from small temperature-independent ones to large complex field- and temperature-dependent ones whose most notable example is $CaF_2:Dy^{2+}$. Finally, there are the photochromic ions: La, Ce, Gd, and Tb. The MCD is usually that of small rigidly shifted bands like that of the F center. These ions exist as several species, however, and apparently the isolated, cubic $f^{n-1}\,d$ ground-state species is a relatively minor constituent.

The theory of magneto-optical dichroism will be described with particular reference to localized impurity states. We shall discuss the effect of spin-orbit and vibronic coupling and shall discuss the selection rules imposed by symmetry. The spectra of the individual divalent lanthanides belonging to the first and second class will be presented and broadly interpreted. Finally, in Sec. V, we shall summarize the results and discuss the use of magneto-optical dichroism for altering and detecting changes in level populations.

II. EXPERIMENTAL

The absorption spectra were all measured at temperatures below 2.2 K with magnetic fields produced by superconductive solenoids and a Cary 14 spectrophotometer. The samples were mounted in the bore of the solenoid and both were immersed directly in liquid helium. The cryostat helium well has a 2.5-in.-i.d. neck at the top and is equipped with a 60-mm-i.d. quartz tailpiece having four flat strain-free Spectrosil[15] windows. The helium bath was cooled to below the λ point by pumping, primarily to reduce the noise caused by light scattering of normally boiling helium.

Several superconductive solenoids were wound and used during the course of this study. The earliest coils were wound with Nb-Zr alloy wire and, owing to the superconductive properties and the design of the solenoid, the maximum field obtained was 28 kOe in a longitudinal solenoid. The solenoids were somewhat temperamental when operated in the high H-I region. Nb-Ti alloy has higher critical field and current values than Nb-Zr, and after Nb-Ti wire became available, we wound a split pair coil with 0.010-in.-diam copper-clad Formvar-insulated Supercon T48B wire.[16] The coil can be used for both longitudinal and transverse observation, is small, gives fields up to 35 kOe, and may be easily operated. Therefore, we shall briefly describe its construction and give the coil parameters.

An aluminum form containing the end faces and the center spacer was machined from a single block in order to achieve strength and accurate alignment. The end faces contain a pattern of 0.010-in.-diam holes which were provided so that liquid helium could penetrate to the windings. The form was anodized for insulation and each half was separately layer wound using 6-lb tension. A layer of 0.005-in.-thick fiber glass cloth was used to cover every fourth layer. The fiber glass not only aids in keeping the coil layer wound, but also provides an open path for liquid-helium penetration. The finished coils each contain 1465 turns and they were joined by soft soldering the leads after carefully cleaning the copper cladding and coating them with clean stainless-steel soldering flux. The soldered lead was taped to the coil with Mylar tape. The coil and its dimensions are shown in Fig. 1. The coil constant is 720 Oe/A, which was determined by measuring the Zeeman splitting of the R_1 line of pink ruby whose g values are accurately known.[17] The maximum obtainable field is 35 kOe at 48 A. The current was supplied by a 100-A Kepco current- and/or voltage-controlled power supply. The field was increased in the voltage-controlled mode, and after the desired field was reached the supply was switched to the current-controlled mode. The coil has been accidentally quenched several times and no deleterious effects were found.

Circularly polarized data were obtained by using a Glan-Foucault polarizer and a Soliel-Babinet compensator. The polarizer is contained in a thin compartment

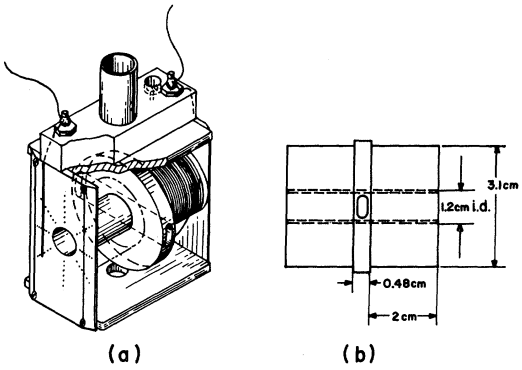

FIG. 1. Split pair of superconductive coils for transverse observation. (a) Sectional view of the solenoid. (b) Plan showing the coil dimensions.

which has been added to the Cary spectrophotometer between the monochromator slit and the beam splitter; thus both sample and reference beams are polarized. The polarizer may be inserted or removed from the main beam and rotated via a shaft which extends through the side wall of the polarizer compartment. The compensator was constructed from a crystal quartz flat and two wedges and has a 1-in.-square clear aperture. The compensator may be attached to the sample compartment wall at the entrance window and the retardation may be set by adjusting a micrometer screw which protrudes through the side wall of the sample compartment.

We usually adjusted the polarizer and compensator to give right circularly polarized light and measured the spectra for magnetic fields pointing in the same (H^+) and opposite (H^-) directions to the direction of light propagation. The field direction is changed by simply reversing the polarity of the leads to the power supply. This is equivalent to keeping the field direction fixed and changing the polarization, but has the advantage that any depolarization arising from the optical elements is identical for the two spectra.

The crystals used were all grown in these laboratories or at the RCA Somerville laboratories by the Czochralski technique. The rare-earth ions were introduced by adding the high-purity LnF_3 to the melt and a seed was pulled in an oxygen-free atmosphere. The crystals were all reduced by heating them in the presence of alkaline-earth metal contained in a sealed quartz ampoule. The heating temperature and time were empirically determined by following the decrease in the narrow-line spectrum of the trivalent rare-earth ion.

III. THEORY

The application of a magnetic field may cause the crystal-field eigenstates to split and to interact, in general. The magnetic contribution to the Hamiltonian is

$$\mathcal{H}=\mu_B(\mathbf{L}+2\mathbf{S})\cdot\mathbf{H}_0, \qquad (1)$$

where μ_B is the Bohr magneton, and $\mathbf{H}_0$ is the externally applied field. The matrix elements of the total angular momentum operator $\mathbf{L}=\sum_i \mathbf{l}_i$ and the total spin operator $\mathbf{S}=\sum_i \mathbf{s}_i$ are expressed here in units of $\hbar$. The application of the magnetic field formally reduces the symmetry group of the impurity. The Zeeman splittings and energy shifts of the impurity levels are at most a few wave numbers for normal values of the magnetic field. Even though the bandwidths of the f^n-f^{n-1} d transitions are usually several hundred wave numbers, large magneto-optical anisotropies are often seen.

Parity-allowed transitions between the magnetic sublevels of two states are induced by the electric field of the incident light wave. The electric field does not act on the electron spin, and photons of a given polarization may only directly change the orbital angular momentum. The orbital moment may vary across a band system and the distribution of orbital moment depends on how the electronic orbital moment is coupled to other momenta. Strong spin-orbit coupling provides a means by which the absorption of different circular polarizations of light depends on the spin. Strong vibronic coupling with nonsymmetric modes leads to a more or less average distribution of orbital momentum across a band, which would mean a small MCD effect. In a band system, in order to have large magneto-optical effects, it is essential that the whole band, or large portions of it, have a single symmetry. The parity-allowed $f^n \rightarrow f^{n-1}$ d transitions are most likely to be accompanied by symmetric modes around the impurity. If the bandwidth is indeed primarily the result of symmetric vibronic coupling, then the band system has the symmetry of the electronic state.[18]

The absorption coefficient for a transition $A \rightarrow B$ induced by the absorption of light of polarization ϵ is

$$\alpha^\epsilon(A,B)=K\langle\sum_b \sigma_{ab}\,|\,(b\,|\,P^\epsilon\,|\,a)\,|^2\rangle_a, \qquad (2)$$

where the concentration and certain physical constants are contained in K, the summation is over the components b of state B, $\langle\cdots\rangle_a$ represents the thermal average over the ground-state components, and σ_{ab} is the energy of the transition. When dealing with circular polarization, it is convenient to write the moment $\mathbf{P}$ in terms of the complex components

$$P^\pm=\mp e(x\pm iy)/\sqrt{2}. \qquad (3)$$

We shall use the traditional convention for circular polarization that when looking toward the source of light a clockwise rotation of the electric vector about that direction is right circular polarization (RCP).[19] We shall use $\epsilon=+$ to refer to RCP, and $\epsilon=-$ to refer to left circular polarization (LCP). The difference between the absorptivity for RCP and LCP light is a measure of the MCD and is referred to as the ellipticity. The mean ellipticity, the difference divided by the sum,

$$\tilde{\Theta}=(\alpha^+-\alpha^-)/(\alpha^++\alpha^-), \qquad (4)$$

is a convenient measure, since it is independent of concentration and thickness and may therefore be directly obtained from the experimentally measured optical densities. In general, $\tilde{\Theta}$ is a function of wave number, temperature, and magnetic field.

The impurity ion has the symmetry of one of the point groups and we may obtain selection rules for the transitions by considering the symmetry transformations of the wave functions and of the dipole moment operator P. The eigenstates of the system are $|\alpha_i\Gamma_i\mu_i)$, where Γ_i is one of the irreducible representations, μ_i is the component label, often called the crystal quantum number, or magnetic substate, and α_i stands for all the other labels needed to characterize the state i. The dipole moment operator P^ϵ transforms according to some representation Γ_P and the polarization is specified by μ_P. The transition dipole moment for the transition $a\rightarrow b$ is given by the generalized Wigner-Eckart theorem[20]

$$(\alpha_B\Gamma_B\mu_b \mid P(\Gamma_P,\mu_P) \mid \alpha_A\Gamma_A\mu_a) = \sum_\beta (d_B)^{-1/2}(\Gamma_A\mu_a\Gamma_P\mu_P \mid \beta\Gamma_B\mu_b)^* \times(\alpha_B\Gamma_B \mid\mid P(\beta\Gamma_P) \mid\mid \alpha_A\Gamma_A). \quad (5)$$

The index β denotes the number of times the representation Γ_B is contained in the product $\Gamma_A\times\Gamma_P$. The polarization dependence is given entirely by the coupling coefficient $(\Gamma_A\mu_a\Gamma_P\mu_P \mid \Gamma_B\mu_b)^*$ if $\Gamma_A\times\Gamma_P$ contains Γ_B only once, which is the most common case, and we need not be at all concerned with the reduced matrix element. Of course, a complete interpretation of a given spectrum consisting, in particular, of overlapping bands, may require a knowledge of at least the relative values of the strengths, which are given by $(\alpha_B\Gamma_B \mid\mid P(\Gamma_P) \mid\mid \alpha_A\Gamma_A)^2$. A model, or some approximation for the electronic coupling scheme, is chosen for that purpose.

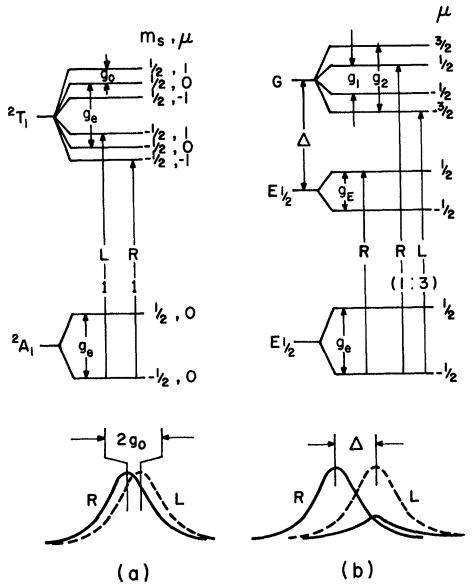

FIG. 2. Magnetic field splittings of group-O_h states $^2A_1$ and $^2T_1$ with (a) no spin-orbit coupling, (b) spin-orbit splitting of $^2T_1$ included. The circularly polarized transitions and their relative strengths from the lowest Zeeman level are indicated by the arrows. The corresponding polarized bands showing the appropriate splittings are shown at the bottom.

TABLE I. Normalized coupling coefficients for $E_{1/2}\times T_1 = E_{1/2}+G$ for the group O.

$E_{1/2}$	T_1		$E_{1/2}$		G			
μ	μ_p	μ'	$\frac{1}{2}$	$-\frac{1}{2}$	$\frac{3}{2}$	$\frac{1}{2}$	$-\frac{1}{2}$	$-\frac{3}{2}$
$\frac{1}{2}$	1				1			
$\frac{1}{2}$	-1			$(\frac{2}{3})^{1/2}$			$(\frac{1}{3})^{1/2}$	
$-\frac{1}{2}$	1		$-(\frac{2}{3})^{1/2}$			$(\frac{1}{3})^{1/2}$		
$-\frac{1}{2}$	-1							1

The divalent lanthanides in CaF_2, except for the photochromic ions, have the O_h symmetry of the Ca^{2+} site. These studies support this model. The dipole moment operator $\mathbf{P}$ transforms like T_{1u} and the magnetic moment $\mathbf{L}+2\mathbf{S}$ transforms like T_{1g} in O_h. Application of a magnetic field splits the degenerate species Γ into magnetic sublevels characterized by μ. We shall illustrate the use of symmetry by considering the MCD of an O_h group $^2A_{1g}\rightarrow{}^2T_{1u}$ transition in two coupling limits: no spin-orbit coupling, and with strong spin-orbit coupling.

A magnetic field splits the states as shown in Fig. 2. The case of no spin-orbit coupling is shown in Fig. 2(a), where the electron-spin g value g_e is the same in both ground and excited states. The orbital g value is taken to be g_0, and the pair of quantum numbers m_s, μ, shown to the right of Fig. 2(a), specifies the levels. Transitions are allowed only between components having the same value of m_s. There are two circularly polarized, equal-intensity transitions for each value of m_s, since

$$(A_{1g}T_{1u}1 \mid T_{1g}1)^2 = (A_{1g}T_{1u}-1 \mid T_{1g}-1)^2.$$

We have shown only the transitions from the $m_s=-\frac{1}{2}$ level, but the transitions from $m_s=\frac{1}{2}$ to $m_s=\frac{1}{2}$, μ have the same polarization and energies as those indicated for $m_s=-\frac{1}{2}$, μ. The polarized spectrum consists of two rigidly shifted bands separated by $2g_0$ and is independent of the temperature. If the bandwidth were very much larger than the Zeeman splitting, the effect would be small and difficult to measure.

We shall now consider strong spin-orbit coupling. The splitting pattern is shown in Fig. 2(b), which shows $^2T_{1u}$ split by spin-orbit interaction into two states G_u and $E_{1/2u}$ having a separation of Δ. The Zeeman splittings of the excited states are determined by the various g values and we have arbitrarily taken the order shown by the values of μ given to the right. The ground-state splitting is, of course, the same as that for no spin-orbit coupling; however, we label the state according to its double-group representation $E_{1/2g}$. The relative intensities of the components of the two transitions are given

TABLE II. Classification of divalent lanthanide ions in fluorite structure host crystals.

Ion	N	Type[a]	Ground state[b]	Remarks
La	1	P		Spectrum not shown
Ce	2	P		Spectrum not shown
Pr	3	K	f^{3}-$^4I_{9/2}$-G	
Nd	4	N	f^{4}-$^5I_4$-A_1[c]	Spectrum not measured
Pm	5	...		Radioactive isotopes, not studied
Sm	6	N	f^{6}-$^7F_0$-A_1	
Eu	7	K	f^{7}-$^8S_{7/2}$	
Gd	8	P		Spectrum not shown
Tb	9	P		Spectrum not shown
Dy	10	N	f^{10}-$^5I_8$-E	
Ho	11	K	f^{11}-$^4I_{15/2}$-$E_{1/2}$	
Er	12	N	f^{12}-$^3H_6$-E[c]	
Tm	13	K	f^{13}-$^2F_{7/2}$-$E_{5/2}$	
Yb	14	N	f^{14}-$^1S_0$-A_1	Spectrum not measured

[a] P is the photochromic ion, K is the Kramers ion, N is the non-Kramers ion.

[b] We give the electron configuration, followed by the lowest Russell-Saunders level, followed by the ground-state symmetry species for the ion in CaF_2.

[c] These ground levels have not been experimentally determined; rather, they are the calculated ones for cubic symmetry given in Ref. 24.

by the coupling coefficients for $E_{1/2}\times T_1$ and these are given in Table I. We shall drop the subscripts g and u and use the group-O coefficients. The polarization is RCP for $\mu_P=1$ and LCP for $\mu_p=-1$. If $g_e\mu_B H\gg kT$, there is one RCP transition to $E_{1/2}$ and the transition to G has two components having the intensity ratio LCP/RCP=3/1. If Δ were much larger than the Zeeman splittings, but smaller than the bandwidth so that the spin-orbit splitting would not be resolved in the zero-field spectrum, the application of a magnetic field would cause the band to develop a distinct asymmetry. The polarized light tends to preferentially pick out certain portions of the band in this case. We have shown qualitatively how the bands appear at the bottom of Fig. 2 and we have taken the over-all intensity of $E_{1/2}\rightarrow G$ to be $\frac{4}{3}$ times that of $E_{1/2}\rightarrow E_{1/2}$ only for illustrative purposes. There is no *a priori* relation between the intensities; that information is given by the reduced matrix elements, which in turn depend on the electronic wave functions. At higher temperatures, transitions from $\mu=\frac{1}{2}$ become important and the bands become composite and show the effects of the small Zeeman splitting.

The analysis we have given is applicable to the MCD of F centers in alkali halides. Margerie and Romestain[21,22] used a free-ion ^2S, ^2P model for the F center; but since the cubic field does not split S or P states, their results are identical with those discussed here. In both cases, the symmetry properties are the same, and it is they that determine the nature, but not the details of the induced MCD.

A complication that sometimes needs to be considered is that the magnetic field may mix states. In our example, if $\mu_B H$ were comparable to Δ, the $E_{1/2}$ and G excited states would mix and intensity would be borrowed one from the other. The off-diagonal mixing is the sole cause of MCD for nondegenerate states and generally is the predominant source of MCD for the even-numbered electron configurations.

Henry, Schnatterly, and Slichter[23] have discussed the analysis of broad-band MCD by use of the method of moments. The method is particularly useful when dealing with a well-defined band shape and bands containing one or two different electronic contributions, and because of the complexity of the electronic states and of the spectra, we do not use the method here. The discussion of the observed MCD of the individual ions which follows is based almost entirely on symmetry considerations. In most cases, the ground-state symmetry and g values are known and the observed MCD and its field and temperature dependence enables us to assign the symmetry species of some of the excited states. We know too little about the excited-state coupling to allow a more detailed analysis of the bands to be made at this time, but we are confident that further MCD studies will do much to elucidate the coupling. The MCD found for the photochromic ions La, Ce, Gd, and Tb provided some of the earliest firm evidence that those ions did not have simple localized f^n or f^{n-1} d ground configurations.

IV. SPECTRA OF INDIVIDUAL DIVALENT LANTHANIDE IONS

We have grouped the ions into three classes which we shall discuss in turn: (a) the photochromic ions; (b) ions having an odd number of electrons (Kramers ions); and (c) ions having an even number of electrons (non-Kramers ions). We have given the classification

and the ground-state assignment of the divalent lanthanide ions in Table II. The states of class (b) ions are all degenerate owing to time-reversal symmetry and they are all split by magnetic fields. The MCD spectra depend on H_0 and T and show large anisotropies. Class (c) ions show a variety of effects ranging from zero as for $CaF_2:Er^{2+}$ to large, complex effects as for $CaF_2:Dy^{2+}$.

We did not study Pm^{2+}, Nd^{2+}, or Yb^{2+} at all. Pm^{2+} has only short-lived isotopes and we found that $CaF_2:Nd^{2+}$ was difficult to produce; the trivalent state of neodymium seems to be particularly resistant to reduction. Nd^{2+} in CaF_2 is expected to have the nondegenerate A_{1g} state lowest and there are no nearby states,[24] so the magneto-optical effects are expected to be small in any case.

A. Photochromic Ions: La^{2+}, Ce^{2+}, Gd^{2+}, and Tb^{2+}

Each of these ions in CaF_2 appears to exist in two or more metastable states, each state having a different absorption spectrum. We shall not show the spectra here because they depend on the crystal's history. The spectrum of the thermally stable state of the four ions are all quite similar, and consists of three or four broad, incompletely resolved bands in the visible. The MCD of the bands have small rigid shifts, similar to the F center in alkali halides. The spectra are not those expected for transitions between f^{n-1} d and f^n configuration for either configuration lowest. These centers have been studied by using EPR[25] and optical techniques,[26] which have included the use of polarized light bleaching and magneto-optical dichroism, and they are becoming understood. Most of the rare-earth ions are part of a center involving a nearby F center and this is the photochromic species.[27,28] The isolated cubic symmetry divalent lanthanide is a minority constituent, but there is some evidence[27] that it can be produced along with other species.

B. Kramers Ions: Pr^{2+}, Eu^{2+}, Ho^{2+}, and Tm^{2+}

Pr^{2+}

The lowest Russell-Saunders level is $^4I_{9/2}$ and the lowest crystal-field component is a fourfold G species.[29] The MCD taken with H_0 along [111] is shown in Fig. 3.

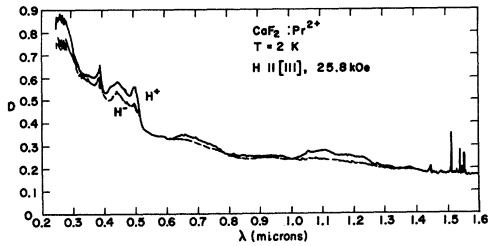

FIG. 3. MCD spectra of $CaF_2:Pr^{2+}$ with $H \parallel [111]$. D denotes optical density, $\ln(I_0/I)$, in this and the other figures.

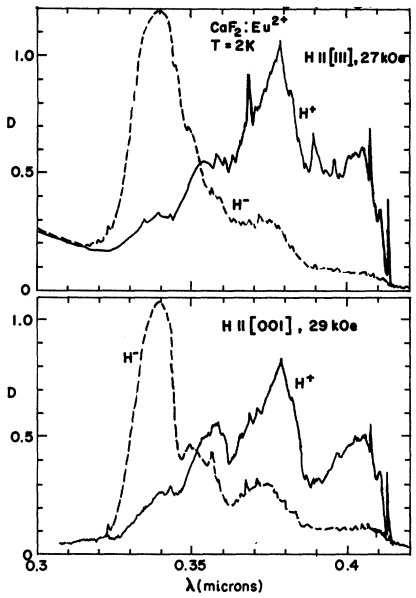

FIG. 4. MCD spectra of $CaF_2:Eu^{2+}$; top $H \parallel [111]$, bottom $H \parallel [001]$.

The most pronounced effect is that most of the bands are stronger for RCP. There are some small shifts in peak positions, but the generally weaker LCP spectrum closely resembles the RCP one. The band near 0.67 μ is an exception and is stronger in LCP than in RCP. We find that Θ depends linearly on H_0 over the range 10–25 kOe.

The MCD spectrum of $CaF_2:Pr^{2+}$ is one of the most complicated cases to analyze because the ground state is a G species. Since $G \times T_1$ contains all three double-group representations, transitions to all states are symmetry allowed. Furthermore, since $G \times T_1$ contains G twice, the relative strengths of $G\mu \rightarrow G\mu'$ transitions depend on the relative values of the reduced matrix elements as well as on the coupling coefficients for $\beta = 1$ and 2, according to Eq. (5). The four ground-state Zeeman levels have unequal spacing, and for $H_0 \parallel [111]$ the energies[29] are $\pm 0.97 \mu_B H_0$ and $\pm 1.38 \mu_B H_0$. The lowest pair of levels, separated by only $0.41 \mu_B H_0$, give the main contribution to the MCD spectrum we measured. We have insufficient information to characterize the levels according to definite values of μ, so we can make no use of coupling coefficients.

We expect that the MCD spectrum would be anisotropic, since the ground-state splitting is. The angular anisotropy and the temperature dependence is a potentially rich source of information about the eigenstates of Pr^{2+}.

Eu^{2+}

The spectrum of $CaF_2:Eu^{2+}$ contains bands at 2200 and 3600 Å. The low-energy band splits into a series of narrow components having a sharp line at the origin

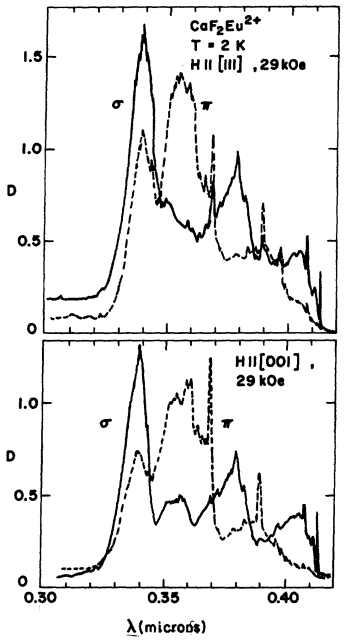

FIG. 5. Magnetic linear dichroism spectra of CaF_2:Eu^{2+}; top $H \parallel [111]$, bottom $H \parallel [001]$. π denotes polarization with the electric vector of the light parallel with the external magnetic field and σ denotes perpendicular polarization.

at 4130 Å. The ground state is $4f^7$-$^8S_{7/2}$, which is split into three components separated by about 0.1 cm^{-1} by the crystal field.[30] The MCD and Faraday rotation in the neighborhood of the 4130-Å line has been studied in weak fields[8] and the MLD was measured in high fields,[9] up to 140 kOe. The rotation was found to be proportional to the magnetization which was used as the basis of an argument[8] for the assignment of the excited state as a weak crystal field ^8P_J of $(4f^6\,5d)$. Later studies showed that the rotation does not sensitively depend on the excited-state coupling[31] and the excited-state configuration was taken to be $(4f^6$-$^7F,\ 5d$-$e)$ although the question is still under discussion.[32]

The MCD spectra for $H_0 \parallel [001]$ and $H_0 \parallel [111]$ shown in Fig. 4 are quite similar to each other. All of the lower-energy components have predominant RCP. The MLD spectra having the same two field orientations are shown in Fig. 5. The spectra are generally similar, the lowest few lines are strongly σ polarized. There are, however, large differences between the spectra for the two field orientations in the region 3500–3700 Å.

The large magneto-optical anisotropies shown are mostly a result of the preferential population of the lowest Zeeman level: $M_J = -\frac{7}{2}$. The ground state does not have pure S character, but contains an admixture[33] of about $0.17\,|\,^6P_{7/2})$. Regardless of the orbital contribution, a $|\,\frac{7}{2}, -\frac{7}{2})$ state is reducible in the group O_h and so group-symmetry selection rules are not much help. We can qualitatively account for the predominance of RCP of the lower-energy components by using the model of $5d$-e_g coupled to the core states $4f^6$-^7F_J. RCP transitions from the ground Zeeman state $|\,\frac{7}{2}, -\frac{7}{2})$ are allowed to M_J components $-\frac{5}{2} \pm pn$ and LCP transitions are allowed to $M_J = -\frac{9}{2} \pm pn$, where p is 0, 1, ..., and n is the rotation axis symmetry about the magnetic field direction. If we ignore f-d interaction, the excited-state energies are proportional to the core J values; therefore there are more low-valued total M_J components at low energy, which favors RCP transitions.

One can, in fact, readily calculate the relative strengths of the transitions of the various states using this coupling scheme. Neglecting f-d interaction, the excited-state energies are the spin-orbit energies

$$E_J = \sum_{x=0}^{J} (x)$$

of the Russell-Saunders core ^7F_J. We may express the ground state in terms of the coupling scheme $|f^6\,^7F_J)\,|fm_l m_s)$ and obtain the dipole moment as the sum of products of coupling coefficients times $(d-e\,|\,\mathbf{P}\,|\,fm_l)$. The calculations show that RCP is strongly favored over LCP and σ over π for $J = 0, 1, 2$; whereas LCP is stronger than RCP and π is stronger than σ for $J = 5$ and 6.

The weak f-d coupling model has been used in order to explain the polarized reflectivity of EuO [34] and to explain the ladder structure of the first band of EuF_2.[31] The model is not really justified on the basis of known free-ion electrostatic F_k and G_k parameters. Interpolation between the known values[35] for Ce^{2+}, Pr^{2+}, and

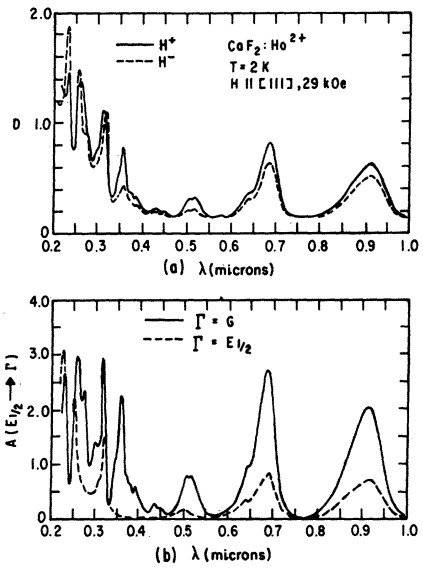

FIG. 6. Spectra of CaF_2:Ho^{2+} with $H \parallel [111]$: (a) MCD spectra; (b) spectra of the G and $E_{1/2}$ excited states derived from the MCD data.

TABLE III. Normalized coupling coefficients for $(E_{5/2}\mu, T_1 1 \mid \Gamma\mu)$.

(A) [001] z-axis quantization

	$E_{5/2}$		G		
$E_{5/2}\times T_1$	$\frac{5}{2}$	$-\frac{5}{2}$	$\frac{3}{2}$	$\frac{1}{2}$	$-\frac{1}{2}$	$-\frac{3}{2}$
$\mid \frac{5}{2}) \mid 1)$					-1	
$\mid -\frac{5}{2}) \mid 1)$	$-\sqrt{\frac{2}{3}}$					$1/\sqrt{3}$

(B) [111] z-axis quantization

	$E_{5/2}$		G			
$E_{5/2}\times T_1$	$\frac{1}{2}$	$-\frac{1}{2}$	$\frac{3}{2}$	$\frac{1}{2}$	$-\frac{1}{2}$	$-\frac{3}{2}$
$\mid \frac{1}{2}) \mid 1)$			$-\frac{1}{3}$			$\frac{2}{3}\sqrt{2}$
$\mid \frac{1}{2}) \mid 1)$	$-\sqrt{\frac{2}{3}}$			$1/\sqrt{3}$		

Yb^{2+} yields values which are certainly not "small" compared with the core spin-orbit parameters. We have calculated eigenvalues by using the complete matrices for spin-orbit and electrostatic f-d interactions for a range of parameters. We find that one can obtain an excellent fit to the two g values of the 4130-Å line, as well as acceptable fits to the energies and relative polarized intensities for F_2 and G_1 parameters about one-tenth of the free-ion values. We shall discuss these results and their implications fully in a separate paper.[36]

Ho^{2+}

The MCD spectrum of CaF_2:Ho^{2+} with H_0 along [111] is shown in Fig. 6(a). The dichroism is quite large and all of the visible and ir bands absorb RCP more strongly than LCP. The MCD of the visible bands have been measured and briefly discussed by Inari[11] and Alekseyeva *et al.*[10] They conclude that both the 5000- and 7000-Å bands have upper states with G character. We agree with this assignment for the former band but find that the 7000-Å band has an appreciable mixture of both $E_{1/2}$ and G upper states.

The ground state is $E_{1/2}$, the g value is -5.9, and in a magnetic field $\mu=\frac{1}{2}$ is the lowest level.[37] Transitions from this level are predominant for $g\mu_B H > kT$. Ho^{2+} has the symmetry structure of the example discussed in Sec. III and the required coupling coefficients are given in Table I. RCP light induces transitions from $\mid E_{1/2}\,\frac{1}{2})$ only to G states and $\mid E_{1/2}\,\frac{1}{2}) \rightarrow \mid G\mu)$ transitions are three times more intense for RCP than for LCP. The observed polarized absorption coefficient is

$$\alpha^{\pm} = (\alpha_{1/2}{}^{+} e^{\mp x} + \alpha_{-1/2}{}^{+} e^{\pm x})\,(2\cosh x)^{-1}, \qquad (6)$$

where the upper sign is used throughout for RCP and the lower sign for LCP. $\alpha_{1/2}{}^{+}$ is the absorption coefficient for RCP transitions from $\mid E_{1/2}\,\frac{1}{2})$, $\alpha_{-1/2}{}^{+}$ is that for RCP transitions from $\mid E_{1/2}-\frac{1}{2})$, and $x=g\mu_B H/2kT$. We may express the absorption coefficients $\alpha_{1/2}{}^{+}$ and $\alpha_{-1/2}{}^{+}$ in terms of the total unpolarized absorbance of $E_{1/2}\rightarrow G$ transitions (A_G) and that of $E_{1/2}\rightarrow E_{1/2}$ transitions (A_E), if we ignore the Zeeman splittings and use Eqs. (2) and (5) and Table I. We find

$$\alpha_{1/2}{}^{+} = \tfrac{1}{4}A_G, \qquad \alpha_{-1/2}{}^{+} = \tfrac{1}{12}A_G + \tfrac{1}{3}A_E. \qquad (7)$$

We may partition the spectrum into the spectra of A_G and A_E by using the measured values of $\tilde{\Theta}$, α, and x in Eqs. (4), (6), and (7), and the results are shown in Fig. 6(b). The 9150-Å band contains both E and G bands which have no measurable splitting. The 6900-Å band is composed of both E and G bands which are split by some 40 cm^{-1} with E lowest. The weak high-energy component of the band is almost all G. The 5000-Å band consists of two G bands and has no E character.

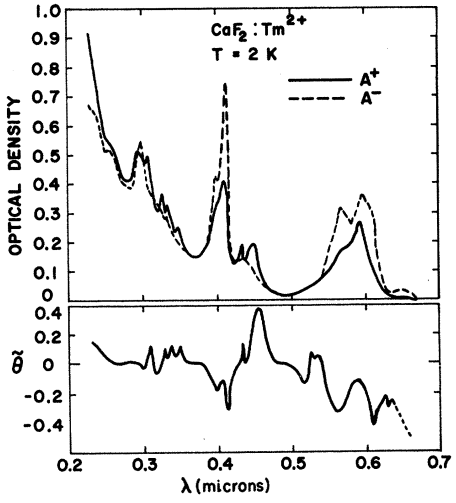

FIG. 7. MCD spectra of CaF_2:Tm^{2+} obtained by extrapolation to $H/T\rightarrow\infty$. A^{+} refers to RCP, A^{-} refers to LCP, and $H \parallel [111]$. The corresponding ellipticity $\tilde{\Theta}$ is shown at the bottom.

Tm^{2+}

The first study that we made on MCD was that of CaF_2:Tm^{2+} and the spectrum was analyzed[6] along the

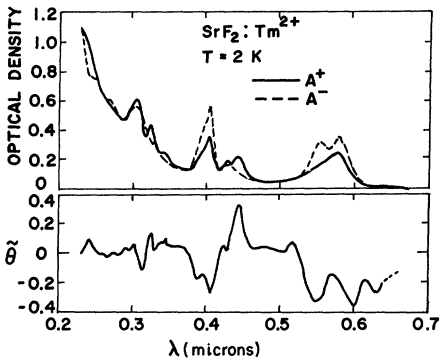

FIG. 8. MCD spectra of SrF_2:Tm^{2+} obtained by extrapolation to $H/T\rightarrow\infty$; other conditions are the same as for Fig. 7.

lines just discussed for Ho^{2+}. The MCD data were used in a Kramers-Kronig analysis and the calculated Faraday rotation dispersions were found to be in good agreement with those experimentally determined[8] for Tm^{2+} in CaF_2 and SrF_2.

Tm^{2+} in the cubic symmetry of the fluorites has the ground state $^2F_{7/2}$-$E_{5/2}$ with a g value close to 3.4. The lowest-energy Zeeman component is $|E_{5/2},-\frac{5}{2})$ for [001] quantization, and $|E_{5/2},-\frac{1}{2})$ in [111] quantization. The coupling coefficients of $E_{5/2}\times T_1$ for both quantization axes are shown in Table III. For magnetic fields along either [001] or [111], RCP transitions from the lowest Zeeman level are allowed to both $E_{5/2}$ and G states, whereas RCP transitions from the upper Zeeman level are allowed only to G states. If we ignore small differences in the energies of transitions to different Zeeman components of G, we see that for either quantization RCP transitions from the upper $E_{5/2}$ level have three times the strength of RCP transitions from the lower $E_{5/2}$ level. The calculated MCD

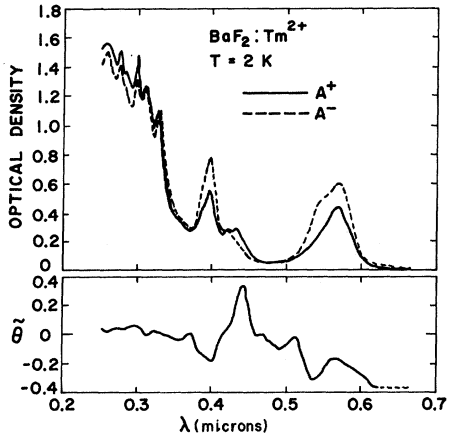

FIG. 9. MCD spectra of BaF_2:Tm^{2+} obtained by extrapolation to $H/T\rightarrow\infty$; other conditions are the same as for Fig. 7.

spectra, $\alpha_\mu{}^+$ of Tm^{2+} in CaF_2, SrF_2, and BaF_2, are shown in Figs. 7–9. The measured curves were fitted to an expression such as Eq. (6) in order to obtain the calculated spectra and

$$\alpha^+(x=\infty)=\alpha_{-1/2}{}^+=\tfrac{1}{3}A_{E5/2}+\tfrac{1}{12}A_G,$$

$$\alpha^-(x=\infty)=\alpha_{1/2}{}^+=\tfrac{1}{4}A_G.$$

The mean ellipticity $\tilde{\Theta}$ is shown on the lower part of each figure. The strong bands near 4000 and 6000 Å have mostly G character, although the lower-energy component of the 6000-Å band has appreciable $E_{5/2}$ character. The weak band near 4200 Å has almost all $E_{5/2}$ character. The predominance of G bands is not surprising in view of the fact that the excited $f^{12}d$ configuration has twice as many G states as $E_{5/2}$ ones.

C. Non-Kramers Ions: Sm^{2+}, Dy^{2+}, and Er^{2+}

Sm^{2+}

Like europium, but unlike the other lanthanides, samarium is quite stable in the 2+ oxidation state and

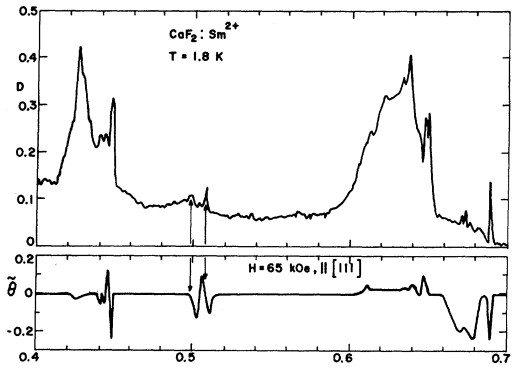

FIG. 10. Absorption spectrum of CaF_2:Sm^{2+} at the top and the ellipticity for $H\parallel[111]$ and 65 kOe at the bottom.

Sm^{2+} has widespread occurrence. The ground configuration is $4f^6$ and Hund's term ^7F is normal ($J=0$ lowest) and split by spin-orbit coupling into seven levels spread over some 5000 cm^{-1}. The next levels above ^7F_J in CaF_2:Sm^{2+} belong to states of f^5d. The resulting low-temperature absorption spectrum has a fairly sharp line at 6905 Å lowest, and is followed by several weaker broader lines and two intense broad but structured bands at 6300 and 4250 Å.

The absorption and fluorescence spectrum have been extensively studied and the MCD was measured by Margerie,[13] who found small field-dependent effects. He showed that the first excited state $^7F_1\,T_{1g}$ at 263 cm^{-1} is mixed with the ground state by the magnetic field, and he gave assignments and g values for several of the narrower bands in the spectrum. The lowest component of f^5d is either A_{1u} or E_u and the next level is T_{1u} and

lies some 116 cm^{-1} higher. The strong 6905-Å absorption line is $f^6(^7F_0)A_{1g}\rightarrow f^5\,dT_{1u}$.

We have measured the MCD throughout the visible spectral range and the spectrum and the MCD at 65 kOe are shown in Fig. 10. Generally the dichroism is small and proportional to H_0. There are two contributions to the MCD having comparable magnitudes; excited-state Zeeman splittings, and mixing of nearby states by the magnetic field. The former causes slightly shifted bands to appear in different polarizations and the latter affects the intensity of the shifted band. The magnetic field mixes $^7F_1$ $T_{1g}0$ with the ground state and the mixing coefficient is

$$\omega=(T_{1g}0\mid S_z\mid A_{1g})\mu_B H_z/\Delta E,$$

whose sign is opposite for H_0 directed along or opposite to the positive z axis. The polarized absorbance is proportional to

$$\mid P^\epsilon(A_{1g}\rightarrow\Gamma)+\omega P^\epsilon(T_{1g}\rightarrow\Gamma)\mid^2,$$

where $P^\epsilon(A_{1g}\rightarrow\Gamma)$ is the transition dipole moment from the ground state and $P^\epsilon(T_{1g}\rightarrow\Gamma)$ is that from the first excited state, for the polarization ϵ. The moments are in phase for one polarization and out of phase for the other. The ellipticity, which is proportional to the difference between the RCP and LCP intensities, depends linearly on H_z and is proportional to the product of ω and the two dipole moments. If the relative values of the dipole strengths are known from experiment, one may determine the magnitude of this contribution to $\tilde{\Theta}$.

If the excited states are themselves appreciably mixed by H_0, the analysis becomes further complicated, since the relative values of the appropriate transition moments are not known. The two relatively weak lines near 5000 Å, indicated by arrows in Fig. 10, give evidence of excited-state mixing, since the S-shaped

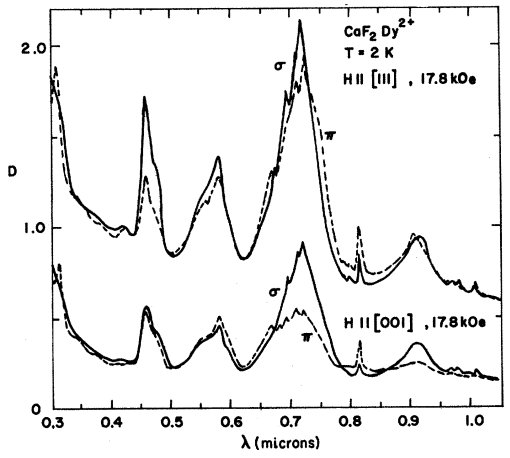

FIG. 11. MLD spectra of CaF_2:Dy^{2+}; top $H\,||\,[111]$, bottom $H\,||\,[001]$.

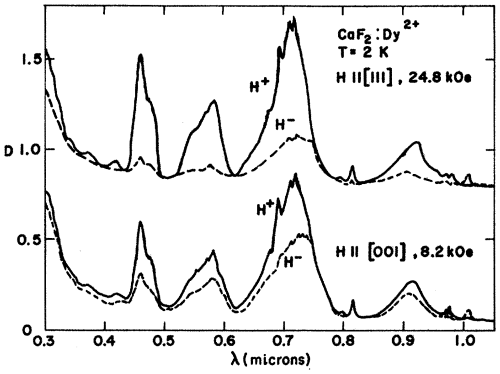

FIG. 12. MCD spectra of CaF_2:Dy^{2+}; top $H\,||\,[111]$, bottom $H\,||\,[001]$.

ellipticities show large shifts from the peak positions of D. These shifts are larger than would be expected for excited-state Zeeman splitting.

Dy^{2+}

The ground configuration of Dy^{2+} is f^{10} and the lowest Russell-Saunders level is $^5I_8$. Zeeman effect[38] and EPR studies[39] have shown that the ground state is a nonmagnetic E_g state and there are two low-lying triplet states; T_{1g} at 4.8 cm^{-1}, and T_{2g} at 28.6 cm^{-1}. The states of $f^9\,d$ begin just above f^{10}-$^5I_6$ and there are broad intense absorption bands extending from the near ir through the uv. A four-level laser emitting at 2.36 μ was operated[40] by pumping in the bands and using a $^5I_7\rightarrow{}^5I_8$ fluorescent transition.

The Faraday rotation in the range 3500–6500 Å has been measured and briefly discussed.[12] The dominant contribution to the rotation was taken to be the mixing of states by the magnetic field. The symmetry- and parity-allowed ground-state transitions are $E_g\rightarrow T_{1u}$ and $E_g\rightarrow T_{2u}$. It was shown that an isolated pair of excited states T_{1u} and T_{2u} which are mixed by the field give opposite contributions to the dichroism. The ground-state mixing and splitting gives important contributions to the magneto-optical effects and they may not be simply interpreted as due to excited-state T_{1u} and T_{2u} mixing.

CaF_2:Dy^{2+} has rather large induced linear dichroism as well as circular dichroism and the effects depend strongly on magnetic field orientation. The MLD with $H_0\,||\,[001]$ and $H_0\,||\,[111]$ are shown in Fig. 11 and the MCD spectra for the same field directions are shown in Fig. 12. It can be seen that the dichroism is quite large and depends on the orientation of H_0. We have not made a detailed study of the field, temperature, and orientation dependence of the magneto-optic effects and shall only qualitatively discuss the spectra.

[001] *transverse.* The MLD is linear in H_0 in all the bands. There is very little splitting of the bands evident; however, a new band appears at 6700 Å in π polarization.

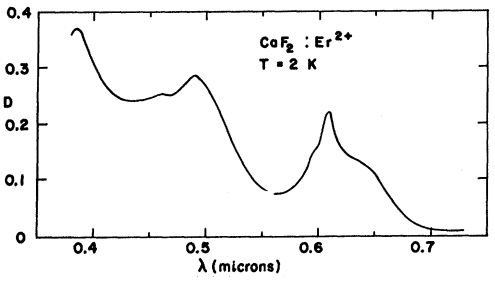

FIG. 13. Absorption spectrum of $CaF_2:Er^{2+}$.

[111] *transverse.* The MLD is nearly linear in H_0 except for the 4500-Å band which shows a greater than linear field dependence. The 9100-Å band has a large splitting with nearly equal intensity components and the σ polarized component lies lower.

[001] *longitudinal.* All the bands except for the 4500-Å one have a linear dependence of Θ on H_0. The 9100-Å band splits and the H^- component is weaker and lies higher in energy than the H^+ component.

[111] *longitudinal.* The field dependence of Θ seems to go from greater than linear for small H_0 to linear for fields above about 8 kOe. Most of the bands appear stronger in H^+ polarization. The 9100-Å band shows a similar dichroism for both **H** along [001] and [111]. The 7200-Å band has a peculiar dichroism effect in both field orientations which seems not to be a result of the optical components or the spectrophotometer. The absorbance is equal for both polarizations going up the long-wavelength side of the band and then the two polarized absorbances abruptly part at 7500 Å, with H^- saturating.

The magneto-optical dichroism must have appreciable contributions of all three possible types; ground- and excited-state Zeeman splitting, mixing of states by the magnetic field, and population effects of the ground Zeeman components. These contributions are sometimes referred to as the A, B, and C terms in expressions for the complex refractive index.[7]

The ground state of $CaF_2:Dy^{2+}$ has no first-order splitting, but the magnetic field splits the nearby T_{1g} state and mixes it with E_g, thus producing a quadratic splitting. The Zeeman shifts are comparable with the zero-field splitting for the fields we used. Examination of the coupling coefficients of $E\times T_1=T_1+T_2$ for different quantization axes reveals that the mixing of the ground state via the field ($\mathbf{H}_0$ transforms like T_{1g}) depends strongly on orientation. The splitting pattern also markedly depends on orientation and so the population effects depend on field orientation. The perturbed E_g ground state in terms of the zero-order [001] basis is

$$|\psi 0)=|E0)+\omega_0|T_10), \qquad |\psi 2)=|E2)+\omega_2|T_22).$$

The splitting is approximately $5(\mu_B H)^2$; therefore for $H_0>15$ kOe and $T<2$ K, the $|\psi 0)$ state is predominantly occupied. The polarized absorbance is the square of the algebraic sum of transition moments from $|E0)$ and $|T_10)$ to the appropriate excited states. The splitting of E_g is smaller for H_0 along [111] and both components of E_g are mixed with both T_{1g} and T_{2g} components. The large induced dichroism is primarily the result of the phase interference between E_g and T_{1g} transition moments.

If the absorption spectrum of transitions from T_{1g} were obtained, it could be used with the ground-state spectrum to deduce excited-state symmetries. The spectrum may be obtained, in principle, from a study of the zero-field spectrum as a function of temperature. We made some measurements using a crude method to produce temperatures above 4 K, but found only small effects. Rather than take differences between separately measured spectra at different temperatures, it would be better to use a temperature-modulation scheme with the detector tuned to the modulation frequency. The T_{2g} spectrum would be very difficult to obtain because T_{2g} lies some 40 K above the ground state and has a very short lifetime. Its contribution to the MCD and MLD is, however, concomitantly smaller than that of T_{1g}.

Er^{2+}

The absorption spectrum of $CaF_2:Er^{2+}$ is shown in Fig. 13. We only studied the spectra in fields up to 15 kOe and no MCD was detected. The absence of an effect is consistent with Er^{2+} having a nonmagnetic E ground state and no nearby states which may be mixed via the magnetic field.[24]

V. SUMMARY AND CONCLUSIONS

We have shown that the magneto-optical effects of the bands due to $f^n\rightarrow f^{n-1}d$ transitions of the divalent lanthanides in CaF_2 may be qualitatively explained on the basis of symmetry considerations. With the exception of the photochromic ions, the spectra are consistent with a model of the divalent lanthanide having the f^n ground configuration, occupying a Ca^{2+} site, and having cubic (O_h) symmetry. The electron spin and orbital momenta are strongly coupled in these configurations, so that the change in orbital momentum caused by electric dipole transitions from a given Zeeman level may be different for the two opposite momenta states of RCP and LCP photons. The magnetic dichroism effects we found are quite large, owing to both population effects among the ground Zeeman levels at low temperature and substantial mixing of states by the applied magnetic field. Entire bands exhibit the same circular dichroism, which we attribute to the fact that the group of excited states comprising the band have the same symmetry and one dominant electronic state. We conclude that the observed bands are predominantly composed of a single electronic excited state broadened by vibronic coupling with totally symmetric modes.

The MCD of the bands of divalent lanthanide ions

are much larger than those of the F centers[21–23] or the transition-metal ions.[7] In the latter two cases spin-orbit coupling is not as strong as in the lanthanides. Furthermore, the transition-metal ion spectra are due to d-d transitions and strong vibrational coupling often plays an essential role in making the transitions allowed. If several different degenerate vibrational modes were coupled with the electronic state, the orbital moment would be scrambled over the vibronic components and the polarizations of the bands in the presence of a magnetic field would be averaged ones.

It has been assumed by many authors[2,5,31,34,41] that the d electron has a large crystal-field splitting, and that the appropriate coupling scheme is one of coupling the f^{n-1} core states with ^2e_g and $^2t_{2g}$ of $5d$. Although our magneto-optical studies have not directly revealed the e_g-t_{2g} splitting, the example of CaF_2:Eu^{2+} gives good support to the coupling scheme. We have calculated polarized component intensities for the magnetic dichroism spectra and the g values of the first excited $f^6\,d$ state which are in good agreement with experiment. We found it necessary to use electrostatic f-d interaction parameters which are only about one-tenth of the expected free-ion values. Although detailed spectral analyses of $f^{n-1}\,d$ configurations are intrinsically difficult because of the large number of states and large core spin-orbit and d crystal-field interactions, it may be possible to treat the f-d electrostatic interaction as a perturbation, if the weakened interaction in crystals should prove to be generally true.

In addition to providing information about the energy levels and transition moment symmetries, the induced magneto-optical dichroism can be used to alter level populations or to detect changes in them. MCD effects of narrow spectral lines have been used to detect population changes in the ground Zeeman levels of neodymium ethylsulfate[42] and in the excited $\bar{E}(^2E)$ state of ruby.[43] Optical pumping experiments on ruby revealed that some ground-state spin memory was retained in the excited states.[44] The ground Zeeman level populations of F centers in KBr were studied by circularly polarized optical pumping of the broad bands in a magnetic field.[45] The MCD of a broad band in CaF_2:Tm^{2+} was used to affect the population distribution in the metastable state $^2F_{5/2}$, $E_{5/2}$ and a high degree of nuclear-spin orientation, as well as electronic-spin memory, was found.[46] The populations in the ground Zeeman levels of Tm^{2+} in both CaF_2 and SrF_2 were actually inverted and a tunable optically pumped maser has been operated.[14] The change in the MCD of CaF_2:Tm^{2+} was also used as a sensitive phonon detector,[47] in an experiment in which phonons were used to induce transitions between Zeeman levels. The use of magneto-optical effects to study phonons and electron-phonon interaction should prove to become increasingly valuable.

ACKNOWLEDGMENTS

We wish to thank C. C. Neil and J. Beherrell for their excellent technical assistance in these studies.

[1] W. Hayes and J. W. Twidell, J. Chem. Phys. **35,** 1521 (1961).
[2] D. S. McClure and Z. J. Kiss, J. Chem. Phys. **39,** 3251 (1963).
[3] D. L. Staebler and Z. J. Kiss, Appl. Phys. Letters **14,** 93 (1969).
[4] H. A. Weakliem and Z. J. Kiss, J. Chem. Phys. **41,** 1507 (1964).
[5] T. S. Piper, J. P. Brown, and D. S. McClure, J. Chem. Phys. **46,** 1353 (1967).
[6] C. H. Anderson, H. A. Weakliem, and E. S. Sabisky, Phys. Rev. **143,** 223 (1966).
[7] A. D. Buckingham and P. J. Stephens, Ann. Rev. Phys. Chem. **17,** 399 (1966).
[8] Y. R. Shen, Phys. Rev. **134,** A661 (1964).
[9] B. P. Zakharchenya and A. Ya. Ryskin, Opt. Spectry. (USSR) **14,** 163 (1963).
[10] L. A. Alekseyeva, N. V. Starostin, and P. P. Feofilev, Opt. Spectry. (USSR) **23,** 140 (1967).
[11] T. Inari, J. Phys. Soc. Japan **25,** 639 (1968).
[12] L. A. Alekseyeva and N. V. Starostin, Opt. Spectry. (USSR) **25,** 532 (1968).
[13] J. Margerie, Physica **33,** 238 (1967).
[14] E. S. Sabisky and C. H. Anderson, IEEE J. Quantum Electron. **QE-3,** 287 (1967).
[15] Thermal-American Fused Quartz Co., Montville, N.J.
[16] Supercon Division National Research Corporation, Natick, Mass.
[17] S. Sugano and I. Tsujikawa, J. Phys. Soc. Japan **13,** 899 (1958).
[18] See, e.g., G. Herzberg, *Electronic Spectra of Polyatomic Molecules* (Van Nostrand, Princeton, N.J., 1967), for a discussion of vibronic coupling.
[19] E. U. Condon and G. H. Shortley, *The Theory of Atomic Spectra* (Cambridge U. P., Cambridge, England, 1957), p. 91.
[20] S. R. Polo, Air Force Cambridge Research Laboratories, Bedford, Mass. Final Report Contract No. AF19 (604)-5541, 1961 (unpublished).
[21] R. Romestain and J. Margerie, Compt. Rend. **258,** 2525 (1964).
[22] J. Margerie and R. Romestain, Compt. Rend. **258,** 4490 (1964).
[23] C. H. Henry, S. E. Schnatterly, and C. P. Slichter, Phys. Rev. **137,** A583 (1965).
[24] K. R. Lea, M. J. M. Leask, and W. P. Wolf, J. Chem. Phys. Solids **23,** 1381 (1962).
[25] C. H. Anderson and E. S. Sabisky, Phys. Rev. B (to be published).
[26] D. L. Staebler, S. E. Schnatterly, and W. Zernik, IEEE J. Quantum Electron. **QE-4,** 575 (1968).
[27] D. L. Staebler, Ph.D. thesis, Princeton University, 1969 (unpublished).
[28] R. C. Alig, Phys. Rev. B (to be published).
[29] F. R. Merritt, H. Guggenheim, and C. G. B. Garrett, Phys. Rev. **145,** 188 (1966).
[30] J. M. Baker, B. Bleaney, and W. Hayes, Proc. Roy. Soc. (London) **A247,** 141 (1958).
[31] M. J. Freiser, S. Methfessel, and F. Holtzberg, J. Appl. Phys. **39,** 900 (1968).
[32] P. Kisliuk, H. H. Tippens, C. A. Moore, and S. A. Pollack, Phys. Rev. **171,** 336 (1968).
[33] J. M. Baker and F. I. B. Williams, Proc. Roy. Soc. (London) **A267,** 283 (1962).
[34] J. Feinleib *et al.*, Phys. Rev. Letters **22,** 1385 (1969).
[35] The data are from: Ce^{2+}: J. Sugar, J. Opt. Soc. Am. **55,** 33 (1965); Pr^{2+}: R. E. Trees, *ibid.* **54,** 651 (1964); Yb^{2+}: B. W. Bryant, *ibid.* **55,** 771 (1965).
[36] H. A. Weakliem (unpublished).

[37] E. S. Sabisky, Phys. Rev. **141,** 352 (1966).
[38] Z. J. Kiss, C. H. Anderson, and R. Orbach, Phys. Rev. **137,** A1761 (1965).
[39] E. S. Sabisky, J. Chem. Phys. **41,** 892 (1964).
[40] Z. J. Kiss and R. C. Duncan, Jr., Proc. IEEE **50,** 1532 (1962).
[41] E. Loh, Phys. Rev. **175,** 533 (1968).
[42] C. K. Asawa and R. A. Satten, Phys. Rev. **127,** 1542 (1962).
[43] S. Geshwind, G. E. Devlin, R. L. Cohen, and S. Chinn, Phys. Rev. **137,** A1087 (1965).
[44] G. F. Imbush and S. Geshwind, in *Optical Properties of Ions in Crystals*, edited by H. M. Crosswhite and H. W. Moos (Interscience, New York, 1967), p. 171.
[45] N. V. Karlov, J. Margerie, and Y. Merle-D'Aubigne, J. Phys. Radium **24,** 717 (1963).
[46] C. H. Anderson and E. S. Sabisky, Phys. Rev. **178,** 547 (1969).
[47] E. S. Sabisky and C. H. Anderson, Appl. Phys. Letters **13,** 214 (1968).

PHYSICAL REVIEW B VOLUME 2, NUMBER 11 1 DECEMBER 197

Dilute Cr^{3+} Paramagnetic Resonance in AlK Alum and $AlNH_4$ Alum*

PHILIP J. BENDT

Los Alamos Scientific Laboratory, University of California, Los Alamos, New Mexico 87544

(Received 13 July 1970)

Single-crystal Cr^{3+} paramagnetic-resonance spectra have been recorded at 1.3 K and ~19 kG for four sulfate alum crystals, in which the Al:Cr ratio varied from 215:1 to 590:1. The g value of the Cr^{3+} ions is independent of crystal orientation, and equals 1.977 ± 0.003. The zero-field Stark splitting $2D$ was measured for AlK alum (Al:Cr=435:1), and equals 0.011 cm^{-1}. The hyperfine coupling constant $|A|$ for ^{53}Cr was measured as $(1.6\pm0.05)\times10^{-3}$ cm^{-1}. The paramagnetic spectra are dominated by the $(-\frac{1}{2}, \frac{1}{2})$ transition, whose linewidth varied from 7 to 22 G. Spin-lattice relaxation is not strongly phonon bottlenecked, and the relaxation time varied from 2 to 3 msec at 0.95 K. With {111} planes perpendicular to the magnetic field, the $(-\frac{1}{2}, \frac{1}{2})$ resonance line is favorable for dynamic pumping of proton polarization.

I. INTRODUCTION

The electron-paramagnetic-resonance (EPR) spectra of Cr^{3+} ions in alums have been calculated and measured at room temperature.[1–3] Better-resolved spectra were obtained by diluting the chromium with diamagnetic aluminum.[2] Bleaney and Penrose[4,5] made measurements down to 20 K. The Cr^{3+} EPR spectra are discussed in two reviews.[6,7]

We have measured the Cr^{3+} EPR spectra of four alum crystals, in which the Al:Cr ratio varied from 215:1 to 590:1, as part of an investigation of the dynamic polarization of protons in alum.[8] The measurements were made in a ^4He cryostat between 1.0 and 1.3 K, and in a magnetic field between 18.5 and 19.5 kG. We measured the Cr^{3+} g value, the zero-field Stark splitting, the hyperfine coupling with the ^{53}Cr nucleus, the ion spin-lattice relaxation times, and the width and shape of the EPR lines. A full account of the polarization experiments is given in the following paper.

II. ALUM CRYSTALS

Single crystals of $AlK(SO_4)_2\cdot12H_2O$ and $AlNH_4(SO_4)_2\cdot12H_2O$ were grown from saturated solutions[9] at room temperature. The concentrations of chromium in the crystals, as determined by analysis,[10] were less than in the solutions, as shown in Table I. Crystals weighing several grams grew from seeds weighing 2–5 mG in about 10 days.

Each crystal was spectrographically analyzed for iron-group impurities. These were present in less than 5 ppm, with one exception: It was reported that $AlNH_4$ alum No. 4 contained approximately the same amount of Cu (100 ppm) as it did Cr. We searched for the paramagnetic Cu^{2+} resonance over a wide range of g values[11] with high sensitivity[12] without finding any indication that copper was present. However, the proton relaxation time was much shorter than in the other $AlNH_4$ alum (crystal No. 3).[13]

The crystal habit is to grow in the form of a regular octahedron, the large plane faces of which are equilateral triangles. The unit cell is cubic and the triangular faces are {111} planes. The angle between normals to adjacent triangular faces is 70° 32′. The density of the crystals was not measured; the handbook values are 1.757 (AlK) and 1.64 ($AlNH_4$).[14]

From the crystals, irregular cylinders were cut which contained two adjacent {111} faces as part of the